



Published in final edited form as:

ACS Appl Mater Interfaces. 2011 May 25; 3(5): 1434–1440. doi:10.1021/am101191d.

Microfluidic fabrication of asymmetric giant lipid vesicles

Peichi C. Hu, Su Li, and Noah Malmstadt

Mork Family Department of Chemical Engineering and Materials Science, University of Southern California Los Angeles, CA 90089

Abstract

We have developed a microfluidic technology for the fabrication of compositionally asymmetric giant unilamellar vesicles (GUVs). The vesicles are assembled in two independent steps. In each step, a lipid monolayer is formed at a water-oil interface. The first monolayer is formed inside of a microfluidic device with a multiphase droplet flow configuration consisting of a continuous oil stream in which water droplets are formed. These droplets are dispensed into a vessel containing a layer of oil over a layer of water. The second lipid monolayer is formed by transferring the droplets through this second oil-water interface by centrifugation. By dissolving different lipid compositions in the different oil phases, the composition of each leaflet of the resulting lipid bilayer can be controlled. We have demonstrated membrane asymmetry by showing differential fluorescence quenching of labeled lipids in each leaflet and by demonstrating that asymmetric GUVs will bind an avidin-coated surface only when biotinylated lipids are targeted to the outer leaflet. In addition, we have demonstrated the successful asymmetric targeting of phosphatidylserine lipids to each leaflet, producing membranes with a biomimetic and physiologically relevant compositional asymmetry.

Keywords

Giant unilamellar vesicles; asymmetric vesicles; microfluidic droplets; lipid bilayer; cell membrane

INTRODUCTION

The chemical composition of the eukaryotic plasma membrane is asymmetric; that is, if the bilayer membrane is considered as two leaflets packed tail-to-tail, the leaflet facing the exterior of the cell contains different lipids at different concentrations than the leaflet facing the interior of the cell.^{1,2} In 1991, Devaux published a classic review of the contemporary understanding of this phenomena; it remains an excellent summary of the early studies that determined the composition in each leaflet.³ There are a number of hypotheses as to the role that membrane asymmetry plays in cell function. Some view certain lipid species as signaling molecules, with their presence in one leaflet or another capable of activating protein machinery. For instance, it has been suggested that the appearance of phosphatidylserine on the outer leaflet is a death signal, serving to recruit phagocytes to attack the dying cell.⁴ It is also possible, however, that asymmetric membranes have special mechanical properties that contribute to cell morphogenesis or vesicle formation.^{3,5} It has also been suggested that long-tailed lipids in one leaflet can interact with lipids on the other leaflet^{6–8}, or that lipid phase structure can be communicated across leaflets^{9–13}, leading to signaling-like transmembrane interactions in asymmetric membranes. The role of membrane asymmetry in cell function remains largely an open question, however.

Synthetic lipid bilayers have traditionally been invaluable tools for studying processes in the cell membrane. These models of the cell membrane can be broadly categorized into five classes: black lipid membranes (BLMs), supported bilayers, liposomes, droplet interface bilayers, and giant unilamellar vesicles (GUVs). BLMs are freestanding bilayer membranes stretched across a circular orifice and supported at their edges by a solvent-mediated interface with a thin solid film.¹⁴ They have been used for fundamental studies of lipid bilayer structure^{15,16} and single-molecule studies of protein electrophysiology.^{17–19} Supported bilayers involve the fabrication of a lipid bilayer upon a solid surface; they have been broadly applied for the display of membrane proteins and biosensing applications.^{20–25} Droplet interface bilayers have been developed only recently, and are formed spontaneously at the contact point of two water droplets in oil.²⁶ Liposomes are used widely in drug delivery applications;^{27,28} they are also important tools for displaying membrane proteins^{29,30} and have been applied in studies of lipid dynamics and phase separation.³¹

None of these synthetic bilayer structures is ideal for studying the full implications of membrane asymmetry, however. Though BLMs, supported bilayers, and droplet interface bilayers can be used to form asymmetric bilayers,^{32,33} they are limited as models of the cell membrane. Supported bilayers introduce artifacts in the diffusive dynamics and phase separation processes of lipid bilayers.^{34–36} These processes are challenging or impossible to observe in BLMs and droplet interface bilayers. Further, none of these approaches is amenable to mechanical testing. Cheng and coworkers recently developed a cyclodextrin delivery-based system for fabricating asymmetric nanoscale liposomes.³⁷ Liposomes, however, have limited applications in analyzing membrane biophysics since their small size makes them unresolvable by optical microscopy and inaccessible to standard mechanical analysis approaches.

This leaves GUVs, spherical lipid bilayer vesicles with diameters in the range of 10–100 μm .^{38,39} GUVs have recently found extensive application as tools for imaging lipid phase separation^{40–45} and observing membrane budding and morphology transformation.^{46,47} They are also classic tools for probing lipid bilayer mechanics⁴⁸ and they have found recent applications in building sensors and engineered surfaces.^{49,50} There are two widely used systems for forming GUVs: electroformation⁵¹ and gentle hydration.⁵² Unfortunately, both of these rely on spontaneous self-assembly of both leaflets simultaneously, and they cannot produce asymmetric membranes. Stachowiak and coworkers recently developed a GUV fabrication technique based on microfluidic jetting; while this method can be performed with asymmetric droplet interface membranes, it is not clear that it is capable of producing asymmetric vesicles.⁵³

A layer-by-layer assembly approach to obtain asymmetric lipid vesicles was originally proposed by Pautot and coworkers.⁵⁴ In their implementation, however, giant vesicles were only obtained when one of the leaflets was constructed from a block copolymer, leading to a structure with minimal biological relevance.⁵⁵ Several groups have followed the approach of Pautot and coworkers in fabricating vesicles in a layer-by-layer process. Yamada and coworkers developed a system for forming symmetric giant vesicles that sit at an oil-water interface.⁵⁶ Hamada and coworkers used a sugar density gradient to fabricate free-floating giant vesicles.⁵⁷ While they have claimed that this approach has the potential to fabricate asymmetric vesicles, they have yet to satisfactorily demonstrate GUV asymmetry. Pontani and coworkers also used a droplet-transfer type system to generate symmetric GUVs containing controllably polymerized actin.⁵⁸ Finally, Tan and coworkers have presented a symmetric lipid vesicle formation technique based on shear-focusing microfluidic droplet generation.⁵⁹

Here, we present a microfluidic flow-based layer-by-layer assembly approach for GUVs that allows for the fabrication of asymmetric membranes in this useful synthetic bilayer format. This work represents the first attempt to quantify the asymmetry of pure lipid membranes prepared in such a format. We demonstrate this asymmetry with both labeled synthetic lipids and natural lipids. This tool promises to be useful for the study of the role lipid bilayer asymmetry plays in plasma membrane phase separation, mechanics, and budding and vesiculation.

EXPERIMENTAL METHODS

Materials

Texas Red-modified 1,2-dipalmitoyl-*sn*-glycero-3-phosphoethanolamine (TR-DPPE), annexin V (Alexa Fluor® 488 conjugate), avidin, and QSY7 carboxylic acid were purchased from Invitrogen (Carlsbad, CA). Biotin-DPPE, 1,2-dipalmitoyl-*sn*-glycero-3-phosphocholine (DPPC), 1,2-dioleoyl-*sn*-glycero-3-phosphocholine (DOPC), cholesterol, and porcine brain L- α -phosphatidylserine (PS) were purchased from Avanti Polar Lipids (Alabaster, AL). Silicon wafers (3 inch (111) mech grade) were obtained from University Wafer (South Boston, MA). SU-8 50 negative photoresist was obtained from MicroChem Corp. (Newton, MA). Poly(dimethylsiloxane) (PDMS) prepolymer and curing agent kits (Sylgard 184) were obtained from Dow Corning (Midland, MI). All other chemicals were purchased from Sigma-Aldrich (St. Louis, MO).

Microfluidic device fabrication

Microfluidic devices were made via standard polymer lithography techniques.⁶⁰ First, a silicon wafer was spin-coated with a 50 μm -thick layer of SU-8 50. A photomask pattern (CAD/Art Services, Inc., Bandon, OR) of microchannels was transferred to the photoresist layer by means of a mask aligner. A second \sim 50 μm thick layer of same photoresist was spin-coated on the previous one and the mask transfer was repeated. After development in ethyl lactate, this negative master wafer was treated with trichloro(perfluorooctyl)silane by vapor deposition for 15 min to facilitate easy detachment of the PDMS replica.

A 10:1 PDMS prepolymer:curing agent mixture was poured onto the master wafer. After curing at 65 $^{\circ}\text{C}$ for 1 h, the PDMS replica was peeled from the master wafer. The PDMS replica and a flat glass (1 mm thick) slide were oxidized by corona treatment (BD-20AC, Electro-Technic Products, Chicago, IL) and bonded irreversibly.⁶¹ The bonded device was then heated at 65 $^{\circ}\text{C}$ for 2 h to recover PDMS surface hydrophobicity. Device geometry is shown in Figure 1.

Asymmetric vesicle fabrication

Asymmetric giant vesicle formation was a two-step process, as shown schematically in Figure 2. First, a two-phase droplet flow was established in a microfluidic channel. The flow was driven by syringe pumps (11 plus; Harvard Apparatus Inc., Holliston, MA). At a 90 $^{\circ}$ channel intersection, an aqueous stream flowing at 20 $\mu\text{L}/\text{h}$ was brought into contact with an oil stream flowing at 100 $\mu\text{L}/\text{h}$, leading to the formation of aqueous droplets in the continuous oil stream. The oil phase consisted of decane containing dissolved lipids. For fluorescence experiments, this oil phase contained 5 mg/mL soy asolectin plus the labeled species as described below. For biotin-DPPE or PS experiments, this phase contained 2.5 mg/mL DOPC, 2.5 mg/mL DPPC and 1.25 mg/mL cholesterol plus biotin-DPPE or PS as described below. The aqueous phase consisted of a sucrose solution (0.5 M sucrose, 10 mM HEPES and 100mM NaCl at pH 7.4).

In a second step, the droplets were dispensed into a vessel with an oil phase (decane:squalene 1:1(v/v)) with lipids. For fluorescence experiments, this oil phase contained 1 mg/mL soy asolectin plus the labeled species as described below. For biotin-DPPE and PS experiments, this phase contained 2.5mg/mL DOPC, 2.5mg/mL DPPC, 1.25mg/mL cholesterol plus biotin-DPPE or PS as described below. This phase was floated above an aqueous phase consisting of a glucose solution (0.5 M glucose, 10 mM HEPES and 100mM NaCl at pH 7.4). This two-phase system was allowed to stabilize for 2 h prior to vesicle formation in order to assure the formation of a stable lipid monolayer at the interface. Droplets were transferred through this monolayer into the water subphase by centrifugation ($200 \times g$) for 2 minutes.

Observing vesicle samples

Microscopic observations of vesicle samples were performed in a Sykes-Moore chamber (Bellco, Vineland, NJ) with #1 cover glass. Glass surfaces were pretreated with liposomes to form fused supported bilayers on the surface.^{62,63} Cover slips were cleaned in acid (sulfuric acid with NoChromix) for 2 h and rinsed with water before drying in a 60 °C oven. A liposome suspension (2 mg/mL asolectin) was made by the standard sonication method.⁶⁴ This suspension was placed on the clean glass for 10 minutes prior to flushing with HEPES buffer (10 mM HEPES and 100mM NaCl at pH 7.4) and adding the vesicle sample.

Spinning disk confocal microscopy was performed using a Yokogawa CSUX confocal head (Tokyo, Japan) on a Nikon TI-E inverted microscope (Tokyo, Japan) with a 60 \times objective (Apo TIRF 1.49 oil immersion). Illumination was provided by 50 mW solid-state lasers at 491, 561, or 640 nm. Brightfield microscopy was performed using the same microscope with transmitted light illumination.

Fluorescence quenching assay

Labeled lipids were included in either the microfluidic channel oil phase (Figure 2a), the stationary oil phase (Figure 2c), or both phases. Each phase was prepared as described above with the addition of TRDPPE to a total concentration of 4 μ g/mL. Vesicles were immediately transferred to an observation chamber where initial fluorescence images were taken. The fluorescent quencher QSY7 carboxylic acid was added to the imaging chamber as a 1 mg/mL solution in the glucose buffer described above. 2 μ L aliquots of this solution were added until further additions resulted in no change in vesicle fluorescence. Quantitative fluorescence comparisons were made using ImageJ (available on the web from NIH: <http://rsbweb.nih.gov/ij/>). Four fluorescence measurements were taken from each vesicle examined; each experimental condition was examined in three vesicles. Measurements were averaged across a given experimental condition and the standard deviation from the mean was propagated as an experimental error. All images were background subtracted such that the field outside of the vesicles was set to an intensity of zero. Lipid flip-flop experiments proceeded in the same fashion, except that the vesicles were first stored at 4 °C for 15 hours.

Asymmetric biotin-binding experiments

Biotin-avidin immobilization of GUVs was performed as described previously.⁶⁵ Briefly, supported bilayers were formed on the glass surface by fusion of liposomes with a 15 wt% biotin-DPPE content. Next, a 25 mg/mL avidin solution was deposited on the bilayer-coated glass and allowed to bind for 15 minutes before being flushed away with HEPES buffer solution.⁶⁶ GUVs were fabricated with biotin-DPPE in either the microfluidic oil phase (Figure 2a) or the stationary oil phase (Figure 2c). Biotin-DPPE was included at 15 wt% of total lipid. The vesicles were introduced to the sample chamber and allowed to bind the avidin-coated surface for five minutes. The chamber was then flushed with buffer solution driven by a syringe pump with flow rate ranging from 0 to 20 mL/hr.

Phosphatidylserine asymmetry

Vesicles were formed with PS either on the outer or inner leaflet. 30 wt% PS (as a fraction of total lipid) was added to either the microfluidic oil phase (Figure 2a) or the stationary oil phase (Figure 2c). The outer leaflet was labeled with biotin-DPPE (15 wt% of total lipid). Then the vesicles were introduced to the avidin-coated sample chamber. Annexin V solution was prepared by diluting a stock solution provided by the vendor 10 times in the glucose solution described above. 25 μ L annexin V solution was added into the sample chamber. The sample was examined 5 minutes after adding the annexin V solution.

RESULTS AND DISCUSSION

Asymmetric giant lipid vesicles were made using a two-step layer-by-layer fabrication process (see Figure 2). The inner leaflet of the asymmetric GUV membrane was established in a microfluidic multiphase flow, as shown in Figure 2a. Droplets of aqueous buffer were formed in a continuous oil phase, which contained dissolved lipid molecules.

The vesicle inner leaflet was formed as a lipid monolayer at the oil-water interface (see inset of figure 2a). The droplets then moved downstream in the continuous oil stream and fell through the outlet on the bottom of the device. To stabilize the first leaflet, we kept the droplets in the same oil/lipid solution used in the microfluidic channel for two hours. During these two hours, droplet size and number remained constant. The droplets did not merge even after several hours.

To form the outer leaflet, a second oil-water interface was established in a microcentrifuge tube. The second lipid monolayer was formed at the interface of a second lipid-oil solution and a glucose buffer. This second oil phase was heavier than the oil phase used in the microfluidic channel in order to minimize lipid mixing. This interface was allowed to stabilize for two hours (see Figure 2c).⁶⁷ The water droplets were then transferred to this oil/water interface (see Figure 2d). Then the tube was centrifuged at $200 \times g$ for 2 min to transfer the water droplets from oil phase to aqueous phase. During the transfer process the outer leaflets of the giant vesicles are formed. Since the droplets contained sucrose solution heavier than the glucose solution in the microcentrifuge tube, the vesicles were stationary at the bottom of the centrifuge tube after centrifugation.

Histograms showing droplet size prior to centrifugation and vesicle size after centrifugation are shown in Figure 3. It is clear from this figure that the larger droplets (diameters greater than about 120 μ m) do not survive the transfer process, and that the smaller droplets (smaller than about 20 μ m) are either transferred across the interface inefficiently or that they merge during the transfer process.

Fluorescently labeled lipids show that lipids from both fabrication steps (Figures 2a and 2d) were incorporated in the final vesicles. Figure 4a shows a vesicle fabricated with labeled lipid only in microfluidic oil phase; Figure 4e shows a vesicle fabricated with labeled lipid only in the stationary oil phase. Clearly, lipids from both phases are incorporated in the vesicle membranes.

Figure 4 also demonstrates vesicle asymmetry in the context of a fluorescence quenching assay. The resonance transfer quencher QSY7 was added to the solution exterior to the vesicle until further additions resulted in no further fluorescence changes. Only accessible Texas red groups were quenched. The asymmetry of the vesicles is clear from Figure 4g. When both leaflets are labeled, about half of the fluorescence is quenched. When the outer leaflet contains the label, about 85% of fluorescence is quenched. When the inner leaflet contains the label, about 15% of fluorescence is quenched. The vesicles are therefore

asymmetric, though not perfectly asymmetric, with about 15% of lipid transferring from one leaflet to the other during the fabrication process.

As seen in Figure 4e (indicated by arrow), about 70% of the vesicles show clear punctate regions of fluorescence heterogeneity. This is likely due to oil inclusions in the bilayer. Oil-free vesicles can be selected visually.

To demonstrate that a variety of lipids can be targeted to the membrane leaflets as desired, we introduced biotin-labeled lipids in either the inner or outer leaflet. The small molecule biotin binds strongly to the protein avidin. Vesicles with biotin on the outer leaflet would be expected to bind to an avidin-coated surface, while vesicles with biotin on the inner leaflet would not (see Figure 5). Vesicle binding to avidin-coated glass was evaluated by introducing vesicles to an avidin-coated surface and then exposing them to an external flow stream. Figure 6(a–c) shows that a vesicle labeled with biotin on the outer leaflet adhered to an avidin-coated glass surface; Figure 6(d–f) shows that a vesicle labeled with biotin on the inner leaflet moved in the flow stream. This experiment was repeated for at least 10 vesicles of each type. All outer-labeled vesicles were immobile at flow rates up to 20,000 $\mu\text{L}/\text{h}$. Inner-labeled vesicles were flushed away at an average volumetric flow rate of $143 \pm 34 \mu\text{L}/\text{h}$. Vesicles with no biotin were flushed away at an average volumetric flow rate of 12 $\mu\text{L}/\text{h}$. These results indicate that biotin groups are significantly more available for binding when they are targeted to the outer leaflet, that inner leaflet lipids generally remain on the inside, and that the vesicles are asymmetric.

To demonstrate that asymmetric vesicles could be made with a natural lipid either on the inner leaflet or outer leaflet, we performed annexin V binding experiments. Annexin V is used as a probe to detect cells with PS exposed on the cell surface.^{68,69} Here, fluorescently labeled annexin V was used to visualize PS. We would expect to observe annexin V binding to vesicles with PS on the outer leaflet, while we would not expect to see such binding with PS on the inner leaflet.

The annexin V binding results are shown in Figure 7. Typical images are shown in Figures 7a and 7b; Figure 7c shows the averaged fluorescent intensity for populations of five vesicles of each type, prepared in a total of six separate fabrication runs (three of each type). Vesicles are clearly asymmetric, with PS appearing on the outer leaflet only when it is specifically targeted there.

To investigate the longevity of these vesicles, TR-DPPE-containing vesicles were stored at 4 °C immediately following centrifugation. Stored vesicles were examined at either 15 hours or 68 hours following fabrication. Figure 8 shows an example of a vesicle from each of these samples. Vesicles with large numbers of oil inclusions (Figure 8b) seemed to last longer, and these vesicles represented almost the entire contents of the 68 hour sample. A vesicle labeled with TR-DPPE on only the outer leaflet from the 15-hour sample was subjected to the fluorescence quenching experiment described by Figure 4. Fifty-one percent of the fluorescence was quenched (compared to 85% quenching for vesicles immediately after preparation). This indicates that lipid flip-flop has led to equilibration of lipids across the membrane. This equilibration time frame is consistent with reported phospholipid flip-flop rates.⁷⁰

CONCLUSIONS

We have demonstrated a two-step microfluidic route to the fabrication of GUVs with compositionally asymmetric bilayers. These structures have potential widespread application in the study of membrane biophysics, including lipid phase separation and membrane mechanics. They also have the potential to serve as biomimetic membranes for more

complex artificial cells. This approach also has potential as a general route to encapsulate arbitrary contents in GUVs; such contents can simply be included in the aqueous phase of the microfluidic flow.

Acknowledgments

This work was supported by the National Institutes of Health under awards 1R21AG033890 and 1R01GM093279.

REFERENCES

- (1). Bretschke M. *Nature-New Biology*. 1972; 236:11-&. [PubMed: 4502419]
- (2). Verkleij AJ, Zwaal RFA, Roelofse B, Comfuriu P, Kastelij D, Vandeene L. *Biochimica Et Biophysica Acta*. 1973; 323:178–193. [PubMed: 4356540]
- (3). Devaux PF. *Biochemistry*. 1991; 30:1163–1173. [PubMed: 1991095]
- (4). Balasubramanian K, Schroit AJ. *Annual Review of Physiology*. 2003; 65:701–734.
- (5). Devaux PF, Herrmann A, Ohlwein N, Kozirov MM. *Biochimica Et Biophysica Acta-Biomembranes*. 2008; 1778:1591–1600.
- (6). Nabet A, Boggs JM, Pezolet M. *Biochemistry*. 1996; 35:6674–6683. [PubMed: 8639617]
- (7). Schram V, Thompson TE. *Biophysical Journal*. 1995; 69:2517–2520. [PubMed: 8599658]
- (8). Stevenson CC, Rich NH, Boggs JM. *Biochemistry*. 1992; 31:1875–1881. [PubMed: 1737040]
- (9). Kiessling V, Crane JM, Tamm LK. *Biophysical Journal*. 2006; 91:3313–3326. [PubMed: 16905614]
- (10). Wan C, Kiessling V, Tamm LK. *Biochemistry*. 2008; 47:2190–2198. [PubMed: 18215072]
- (11). Kiessling V, Wan C, Tamm LK. *Biochimica Et Biophysica Acta-Biomembranes*. 2009; 1788:64–71.
- (12). Collins MD. *Biophysical Journal*. 2008; 94:L32–4. [PubMed: 18096628]
- (13). Collins MD, Keller SL. *Proceedings of the National Academy of Sciences*. 2008; 105:124–128.
- (14). White SH, Thompson TE. *Biochimica Et Biophysica Acta*. 1973; 323:7–22. [PubMed: 4360052]
- (15). White SH. *Biophysical Journal*. 1970; 10:1127-&. [PubMed: 5489777]
- (16). White SH, Chang W. *Biophysical Journal*. 1981; 36:449–453. [PubMed: 7306666]
- (17). Jeon TJ, Malmstadt N, Schmidt JJ. *Journal of the American Chemical Society*. 2006; 128:42–43. [PubMed: 16390112]
- (18). Kasianowicz J, Brandin E, Branton D, Deamer DW. *Proceedings of the National Academy of Sciences*. 1996; 93:13770–13773.
- (19). Malmstadt N, Nash MA, Purnell RF, Schmidt JJ. *Nano Letters*. 2006; 6:1961–1965. [PubMed: 16968008]
- (20). Atanasov V, Knorr N, Duran RS, Ingebrandt S, Offenhausser A, Knoll W, Koper I. *Biophysical Journal*. 2005; 89:1780–1788. [PubMed: 16127170]
- (21). Yang TL, Baryshnikova OK, Mao HB, Holden MA, Cremer PS. *Journal of the American Chemical Society*. 2003; 125:4779–4784. [PubMed: 12696896]
- (22). Knoll W, Frank CW, Heibel C, Naumann R, Offenhausser A, Ruhe J, Schmidt EK, Shen WW, Sinner A. *Reviews in Molecular Biotechnology*. 2000; 74:137–158. [PubMed: 11143794]
- (23). Albertorio F, Diaz AJ, Yang T, Chapa VA, Kataoka S, Castellana ET, Cremer PS. *Langmuir*. 2005; 21:7476–7482. [PubMed: 16042482]
- (24). Jung H, Robison AD, Cremer PS. *Journal of the American Chemical Society*. 2009; 131:1006–1014. [PubMed: 19125648]
- (25). Tanaka M, Hermann J, Haase I, Fischer M, Boxer SG. *Langmuir*. 2007; 23:5638–5644. [PubMed: 17408291]
- (26). Hwang WL, Chen M, Cronin B, Holden MA, Bayley H. *Journal of the American Chemical Society*. 2008; 130:5878–+. [PubMed: 18407631]
- (27). Basu, SC.; Basu, M. *Liposome methods and protocols*. Humana Press; Totowa, N.J.: 2002.

- (28). Torchilin, VP.; Weissig, V. *Liposomes: a practical approach*. 2nd ed.. Oxford University Press; Oxford: 2003.
- (29). Schubert R. *Methods in Enzymology*. 2003; 367:46–70. [PubMed: 14611058]
- (30). Vojta A, Scheuring J, Neumaier N, Mirus O, Weinkauff S, Schleiff E. *Analytical Biochemistry*. 2005; 347:24–33. [PubMed: 16236237]
- (31). Heberle FA, Buboltz JT, Stringer D, Feigenson GW. *Biochimica Et Biophysica Acta-Molecular Cell Research*. 2005; 1746:186–192.
- (32). Montal M, Mueller P. *Proceedings of the National Academy of Sciences of the United States of America*. 1972; 69:3561–3566. [PubMed: 4509315]
- (33). Peterson IR. *Journal of Physics D-Applied Physics*. 1990; 23:379–395.
- (34). Przybylo M, Sykora J, Humpolickova J, Benda A, Zan A, Hof M. *Langmuir*. 2006; 22:9096–9099. [PubMed: 17042516]
- (35). Stottrup BL, Veatch SL, Keller SL. *Biophysical Journal*. 2004; 86:2942–2950. [PubMed: 15111410]
- (36). Seu KJ, Pandey AP, Haque F, Proctor EA, Ribbe AE, Hovis JS. *Biophysical Journal*. 2007; 92:2445–2450. [PubMed: 17218468]
- (37). Cheng HT, Megha, London E. *Journal of Biological Chemistry*. 2009; 284:6079–6092. [PubMed: 19129198]
- (38). Kim S, Martin GM. *Biochimica Et Biophysica Acta*. 1981; 646:1–9. [PubMed: 7272296]
- (39). Oku N, Scheerer JF, Macdonald RC. *Biochimica Et Biophysica Acta*. 1982; 692:384–388. [PubMed: 7171602]
- (40). Feigenson GW, Buboltz JT. *Biophysical Journal*. 2001; 80:2775–2788. [PubMed: 11371452]
- (41). Veatch SL, Keller SL. *Physical Review Letters*. 2002; 89:268101. [PubMed: 12484857]
- (42). Veatch SL, Keller SL. *Physical Review Letters*. 2005; 94:148101. [PubMed: 15904115]
- (43). Veatch SL, Soubias O, Keller SL, Gawrisch K. *Proceedings of the National Academy of Sciences*. 2007; 104:17650–17655.
- (44). Zhao J, Wu J, Heberle FA, Mills TT, Klawitter P, Huang G, Costanza G, Feigenson GW. *Biochimica Et Biophysica Acta-Biomembranes*. 2007; 1768:2764–2776.
- (45). Cans AS, Andes-Koback M, Keating CD. *Journal of the American Chemical Society*. 2008; 130:7400–7406. [PubMed: 18479139]
- (46). Yu Y, Vroman JA, Bae SC, Granick S. *Journal of the American Chemical Society*. 2010; 132:195–201. [PubMed: 20000420]
- (47). Kovačič J, Božič B, Svetina S. *Biophysical Chemistry*. 2010; 152:46–54. [PubMed: 20719426]
- (48). Kwok R, Evans E. *Biophysical Journal*. 1981; 35:637–652. [PubMed: 7272454]
- (49). Zhou J, Loftus AL, Mulley G, Jenkins ATA. *Journal of the American Chemical Society*. 2010; 132:6566–6570. [PubMed: 20405918]
- (50). Chung M, Lowe RD, Chan YHM, Ganesan PV, Boxer SG. *Journal of Structural Biology*. 2009; 168:190–199. [PubMed: 19560541]
- (51). Angelova MI, Soléau S, Méléard P, Faucon JF, Bothorel P. *Progress in Colloid and Polymer Science*. 1992; 89:127–131.
- (52). Adams DR, Toner M, Langer R. *Langmuir*. 2007; 23:13013–13023. [PubMed: 17983248]
- (53). Stachowiak JC, Richmond DL, Li TH, Liu AP, Parekh SH, Fletcher DA. *Proceedings of the National Academy of Sciences*. 2008; 105:4697–4702.
- (54). Pautot S, Frisken BJ, Weitz DA. *Langmuir*. 2003; 19:2870–2879.
- (55). Pautot S, Frisken BJ, Weitz DA. *Proceedings of the National Academy of Sciences*. 2003; 100:10718–10721.
- (56). Yamada A, Yamanaka T, Hamada T, Hase M, Yoshikawa K, Baigl D. *Langmuir*. 2006; 22:9824–9828. [PubMed: 17106968]
- (57). Hamada T, Miura Y, Komatsu Y, Kishimoto Y, Vestergaard M, Takagi M. *Journal of Physical Chemistry B*. 2008; 112:14678–14681.
- (58). Pontani L-L, van der Gucht J, Salbreux G, Heuvingh J, Joanny J-F, Sykes C. *Biophysical Journal*. 2009; 96:192–198. [PubMed: 19134475]

- (59). Tan YC, Hettiarachchi K, Siu M, Pan YP. *Journal of the American Chemical Society*. 2006; 128:5656–5658. [PubMed: 16637631]
- (60). Duffy DC, McDonald JC, Schueller OJA, Whitesides GM. *Analytical Chemistry*. 1998; 70:4974–4984.
- (61). Haubert K, Drier T, Beebe D. *Lab on a Chip*. 2006; 6:1548–1549. [PubMed: 17203160]
- (62). Brian AA, Mcconnell HM. *Proceedings of the National Academy of Sciences of the*. 1984; 81:6159–6163.
- (63). Richter R, Mukhopadhyay A, Brisson A. *Biophysical Journal*. 2003; 85:3035–3047. [PubMed: 14581204]
- (64). Stryer, L. *Biochemistry*. 2nd ed.. W.H. Freeman; San Francisco: 1981.
- (65). Su Li PH, Noah Malmstadt *Analytical Chemistry*. 2010; 82:7766–7771.
- (66). Diamandis EP, Christopoulos TK. *Clinical Chemistry*. 1991; 37:625–636. [PubMed: 2032315]
- (67). Lee JB, Petrov PG, Dobereiner H. *Langmuir*. 1999; 15:8543–8546.
- (68). Koopman G, Reutelingsperger CPM, Kuijten GAM, Keehnen RMJ, Pals ST, Vanoers MHJ. *Blood*. 1994; 84:1415–1420. [PubMed: 8068938]
- (69). Vermes I, Haanen C, Steffensnacken H, Reutelingsperger C. *Journal of Immunological Methods*. 1995; 184:39–51. [PubMed: 7622868]
- (70). Liu J, Conboy JC. *Biophysical Journal*. 2005; 89:2522–2532. [PubMed: 16085770]

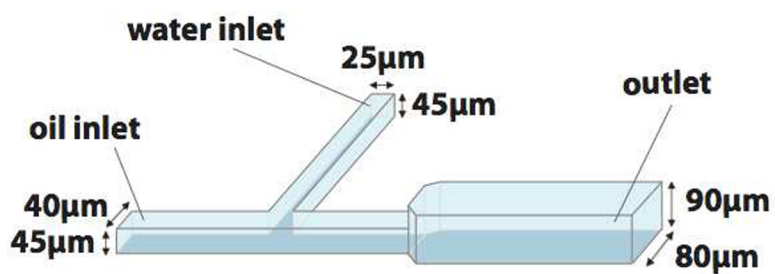


Figure 1. Schematic of the microfluidic channel used for vesicle fabrication. Channels were made in a two-step photoresist patterning process, facilitating two different channel depths. At the inlet, the channels are 40 μm wide by 45 μm deep; after the channel junction, they widen to 80 μm wide by 90 μm deep.

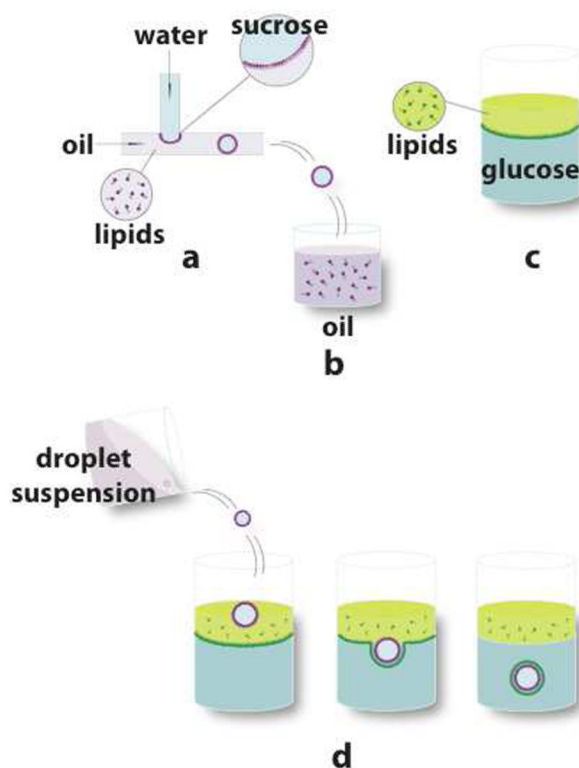


Figure 2. Fabrication scheme for asymmetric GUVs. (a) Droplets of an aqueous solution were formed in an immiscible oil stream at a channel junction; lipids in the oil form a monolayer at the phase interface. (b) Water droplets were dispensed into a vessel. These monolayer-coated droplets were collected in the same oil phase as that used in the device and were allowed to stabilize for at least 2 hours. (c) The second monolayer was formed by allowing lipids at an oil-water interface to stabilize for at least two hours. (d) The water droplets were poured into a vessel with a lipid monolayer at an oil-water interface. Centrifugation was used to force the vesicles through the interface, forming the outer leaflet of the bilayer.

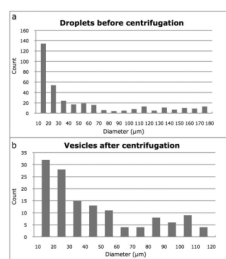


Figure 3. The effect of centrifugation on droplets as they are transferred to the water subphase as vesicles. (a) Histogram of droplet size prior to centrifugation. (b) Histogram of vesicle size after centrifugation. Size measurements were made by hand from phase contrast micrographs.

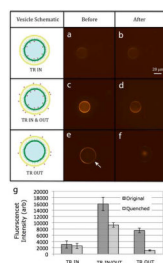


Figure 4.

Fluorescence quenching to demonstrate vesicle asymmetry. The two columns of panels show representative vesicle confocal fluorescence images before (a, c, e) and after (b, d, f) the addition of an energy-transfer quenching agent. This experiment was performed for vesicles with fluorophore only on the inner leaflet (a, b), on both leaflets (c, d), and only on the outer leaflet (e, f). Average fluorescent intensities before and quenching are plotted in (g) for a set of three vesicles of each type. The arrow in (e) indicates a spot of elevated fluorescence likely corresponding to oil retained in the membrane bilayer. Scale bar is 20 μm , and applies to all images. Error bars are \pm one standard deviation.

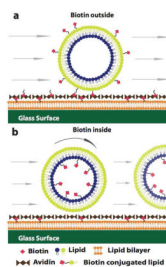


Figure 5. Schematic describing the biotin-avidin binding experiment. (a) Vesicles with biotinylated lipids on the outer leaflet will be anchored to avidin-coated surfaces. (b) Vesicles with biotinylated lipids on the inner leaflet will not bind to the avidin layer.

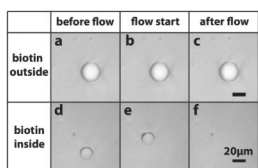


Figure 6.

Results of a biotin binding experiment. Phase-contrast images of a vesicle with biotinylated lipids on either the outer leaflet (a–c) or on the inner leaflet (d–f). (a–c) and (d–f) each represent a time series of images as a flow is initiated in the sample chamber. Each image in a time series represents a 1 s increment. Each scale bar is 20 μm , and applies to all images in the corresponding time series.

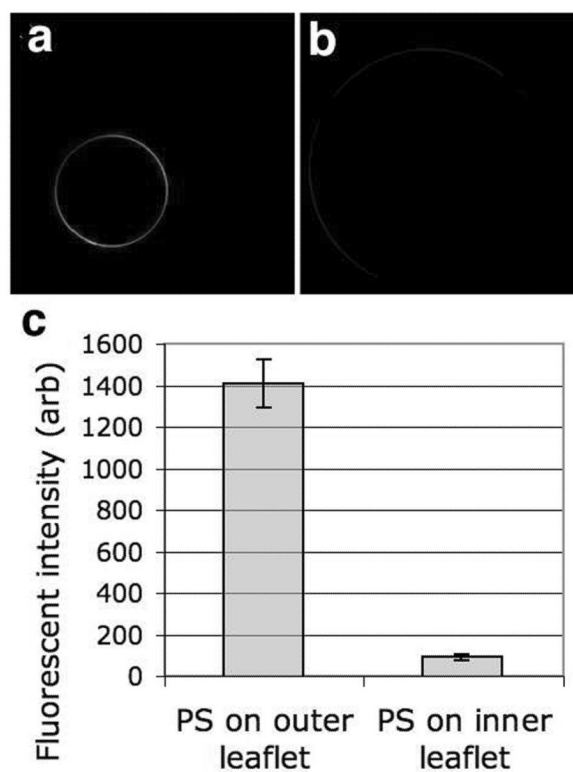


Figure 7. Annexin V binds only to vesicles with PS targeted to the outer leaflet (a) A confocal fluorescence image of annexin V binding to a vesicle containing PS in the outer leaflet. (b) In a similar confocal image of a vesicle with PS in the inner leaflet, annexin V binding is not seen. (c) Fluorescent intensity of annexin V bound to vesicles with PS in either the inner or outer leaflet. Error bars are \pm one standard deviation. For vesicles without PS, the fluorescent intensity was indistinguishable from background.

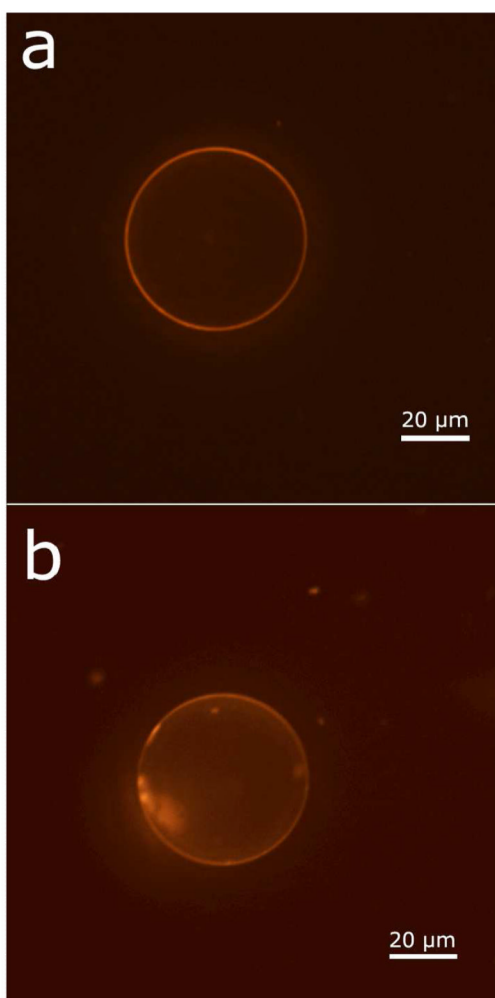


Figure 8. Vesicles images after storage at 4 °C for (a) 15 hours and (b) 68 hours. Scale bars are 20 μm .